IEEE Access
Multidisciplinary | Rapid Review | Open Access Journal

Received April 14, 2022, accepted April 27, 2022, date of publication May 3, 2022, date of current version May 12, 2022.

Digital Object Identifier 10.1109/ACCESS.2022.3172305

Consequences of Flux Gap on Intriguing Features of Modular Stator Inset Permanent Magnet Consequent Pole Synchronous Machine

WASIQ ULLAH[1], (Graduate Student Member, IEEE), FAISAL KHAN[1], (Senior Member, IEEE), SHAHID HUSSAIN[1], (Graduate Student Member, IEEE), FAHAD ALTURISE[2], MUHAMMAD YOUSUF[1], (Graduate Student Member, IEEE), AND SIDDIQUE AKBAR[1]

[1]Department of Electrical and Computer Engineering, COMSATS University Islamabad, Abbottabad Campus, Abbottabad 22060, Pakistan
[2]Department of Computer, College of Science and Arts in Ar Rass, Qassim University, Ar Rass, Qasim 52571, Saudi Arabia

Corresponding author: Wasiq Ullah (wasiqullah014@gmail.com)

ABSTRACT In this paper a novel Inset Permanent Magnet Consequent Pole Synchronous Machine (IPMCPSM) with H-type modular stator core for higher average torque (T_a), torque density (T_d), power density (P_d) and efficiency (η) with features of reduced torque ripple ratio (T_r) and harmonics content in back-EMF (EMF_{THD}) are proposed. Detailed static analysis of the proposed IPMCPSM under variable flux gaps at all and alternate stator teeth is investigated. Performance analyses disclose that with variable flux gaps in proposed IPMCPSM, beside improved flux weakening capability due to flux focusing effects, electromagnetic performance is greatly improved. Additionally, due to physical isolation of the adjacent phase modules with modular topology, mutual flux influence is de-coupled that improve phase self-inductance to mitigate the short-circuited current under fault condition whereas mutual flux decoupling mitigates mutual inductance that ultimately improves overall machine fault-tolerant capability. Furthermore, effectiveness of the proposed IPMCPSM with H-type modular stator is elaborated with comparative study of conventional E-core and C-core topologies. Detailed comparative analysis reveals that proposed IPMCPSM suppresses EMF_{THD}, improve η by 18.9%, diminish T_r up to 55% and boost T_a and P_d maximum up to 2.66, 2.59 times, respectively with enhanced flux focusing effects and fault tolerant capability.

INDEX TERMS AC machines, consequent pole, flux gap, permanent magnet machine, modular stator, H-type stator, modular permanent magnet machine.

I. INTRODUCTION

Flux Switching Machines (FSMs) are double-salient robust machines that offers high-torque and power density therefore, considered as prominent candidate for high-speed brushless AC applications. FSMs incorporates features of Permanent Magnet machines and Switch Reluctance Machine (SRM). Thus, based on PM excitation source, it is classified as Permanent magnet (PM) FSM (PMFSM) [1]. PMFSMs are suitable to Electric Vehicles (EVs), electric propulsion, Hybrid Electric Vehicles (HEV), electric power-assisted steering, electric craft, renewable and automotive and many industrial applications [2].

Due to position of PM as well as design topology, permanent magnet machines differ. In case of PMFSMs, circumferentially magnetized alternate PMs polarities are sandwich between stator and armature coils [3], whereas in case of interior PM synchronous machines (IPMSM), inset PMs rotor are employed. Furthermore, surface-mounted PM machine (SMPMM) deploy PMs on rotor surface.

Considering excitation source, majority of PM excited machines employee's ferrite and rare-earth Sintered Neodymium-iron-boron (NdFeB) PMs however, because of potential surge in PM demand and deficiency of raw-materials, overall machine price greatly rises with PM. This is because of comparatively high quantity of the PM utilization. Considering the PM material supply period volatility, PM machine design optimization with no PM or less PM are noticeable while retaining much of the performance advantage over competing machine types, such as induction machines and synchronous reluctance machines, which tend to have markedly lower torque density [4].

The associate editor coordinating the review of this manuscript and approving it for publication was Jinquan Xu.

In regard of PM utilization and cost-efficient machines, many researchers in the recent years are attracted by consequent pole (CP) on rotor and stator sides. Authors in [5]–[7] reported rotor-CP machine whereas CP-stator are investigated in [8]–[10] and dual modulation (both rotor and stator CP) is reported in [11]. In comparison with rotor-CP and stator-CP, despite of double PM volume utilization, dual modulation machine evident mechanical restriction. Stator-CP exhibits merits of reduced core-losses due to suppression of lower order space harmonics however, due to allotment of phase winding and PM excitation in stator, electrical loadings reduced that deteriorates performance.

Compared to conventional SMPMM, rotor-CP topologies reduce PM volume utilization to half. In rotor-CP structure, either North or South-pole are employed, and the adjacent salient iron pole behaves as virtual South or North-pole. In context of application, due to reduced PM usage, CP structure are preferred in Hybrid excited machines [12], in comparison with PM Vernier machines [13] and flux reversal partitioned stator [14]. Furthermore, rotor radial position and retaining force enhance regulation capability of rotor-CP structure that make it prominent candidate for bearingless PM motor [15]–[17].

Optimization and comparison of fractional slot SMPMM with rotor-CP shows that SMPMM with rotor-CP achieve same performance as fractional slot SMPMM at 33% less PM usage. Moreover, 26% more average torque is achieved in consequent pole permanent magnet flux reversal machine than the existing conventional design [18] whereas author in [19] achieved almost the same output torque as conventional SMPMM that and save approximately one-third of amount of PM. Moreover, author in [20] reported that utilizing CP topology, torque per unit magnet volume machine can be improved by 38% while the output torque is only 8% less than conventional SMPMM.

In regard of IPMSM with consequent pole topology, study reported in [21] demonstrated that output torque can be improved by 2.76% while reducing the PM volume by 20.29%. Keeping the PM volume same, comparative performance analysis of consequent pole modular machines with modular structure inset PM machines is reported in [9] which demonstrated that the higher average torque in consequent pole modular machine is obtained than that of corresponding inset PM machines. It is worth noting that, despite of lower average torque, IPM with consequent pole exhibits reduced torque ripples and cogging torque and improved torque density. This torque density is further improved in hybrid dual PM machines utilized for EVs application [22].

However, despite of rotor-CP mechanical constraint, consequent pole PM machines suffers from intrinsic uni-polar shaft flux leakages accompanied with even-order back-EMF and air-gap flux density harmonics content. This issue is investigated in [23] utilizing multi-layer winding whereas authors in uses hybrid PMs rotors with different magnetization pattern that effectively truncates back-EMF higher order even harmonics and eliminates rotor shaft flux leakages.

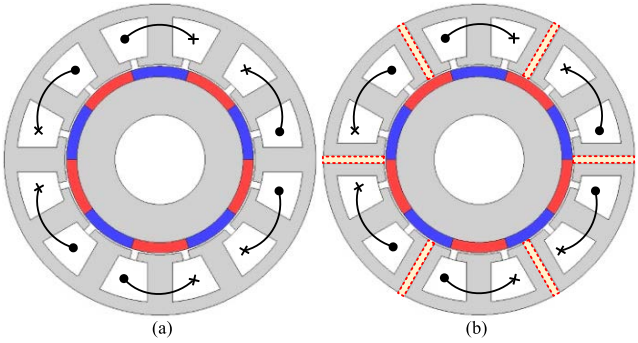

FIGURE 1. Cross sectional view of SMPMM (a) Non-modular stator (b) Modular stator.

Considering stator structure, the above-said topologies are non-modular. In case of modular topologies with segmented stator lamination, despite of improved thermal and mechanical integrity, modular design shows advantages of easy winding process in comparison with non-modular topology. Therefore, offered improved fault tolerant capability with low on-site maintenance. For this purpose, rotor-CP achieved excellent flux-focusing that enhance torque density and suppressed iron bridge flux leakage retaining torque ripples and efficiency [24] whereas rotor-CP with modular stator topology is investigated for low-order space harmonics suppression. Modular stator with through flux gap in the form of E-core structure are investigated in [25] as shown in Figure. 1. Beside high PM usage, performance degrades in E-core stator structure for rotor pole number less than stator slots. It shows positive impact only in case when rotor poles number are greater than stator slots.

Despite of stator-CP machines, modular topologies with segmented PM, segmented rotor and segmented stator lamination have been a research interest. Authors in [26], [27] investigated segmented PM machine whereas segmented inner rotor are discussed in [28]. Analysis reveals that in comparison with stator PM segmentation, rotor segmentation suffers from mechanical constraints under high-speed application. Therefore, stator segmentation is preferred. In this regard, Authors in [29] studies segmented stator PM machine whereas a comparative study of modular stator with conventional machine is analyzed in [30]. It is found that stator segmentation greatly helps in improving fault-tolerant capability of machine due to physical isolation of the stator phase modules [31].

In order to overcomes the aforesaid demerits, in this paper, rotor-CP and modular stator of SMPMM are integrated to develop a novel Inset Permanent Magnet Consequent Pole Synchronous Machine (IPMCPSM) with H-type modular stator core with depicted flux gap at alternate and all stator teeth as shown in Figure. 2 which is an extension of author previous work [32]. It is noteworthy that both all teeth flux gap and alternate teeth flux gap are similar but different in number of flux gaps. In all teeth flux gaps, there are physical isolation of stator at each pole whereas in alternate pole, flux gaps

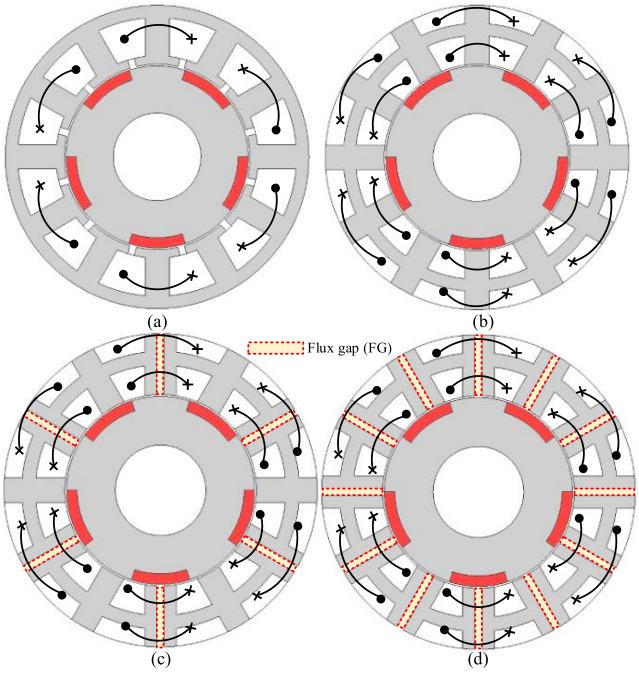

FIGURE 2. Geometric formation of novel H-type stator core (a) Non-modular conventional CP (C) Non-modular proposed H-type stator core (c) Modular H-type stator with alternate teeth flux gap and (d) Modular H-type stator with all teeth flux gap.

are reduced to half and alternate stator pole are physically isolated.

Some of the major contribution of this paper includes development of the proposed IPMCPSM by first converting SMPMM to rotor-CP that reduces PM volume to half and secondly H-type stator topology is formed by introducing flux gap at alternate and all stator teeth as shown in Figure. 2(c-d). Intriguing feature of proposed IPMCPSM modular topology and comparative performance is investigated with varying flux gap width whereas simplified mathematical model is opted to explain working principle as well as back-EMF and torque generation mechanism. Finally, superiority of proposed modular IPMCPSM is justified by detailed comparison of proposed H-type stator with conventional E-core and C-core CP as shown in Figure. 3.

In the following, Section II explains modular stator rotor-CP design and operating principle. Enhancing capability of proposed IPMCPSM is analyzed in Section III. Section IV investigates electromagnetic performance analysis whereas conventional and proposed design is evaluated in section V and finally, some conclusion is drawn in Section VI.

II. MODULAR STATOR ROTOR-CP DESIGN AND OPERATING PRINCIPLE

For the proposed IPMCPSM with H-type modular stator, depicted design parameters are listed in Table 1 and shown in Fig. 4. To avoid local saturation, total active tooth body of stator teeth in stator core is retained same regardless of variation of FGs width. With focus on modular topology, depicted geometric parameters i.e., air-gap, rotor shaft, PM width,

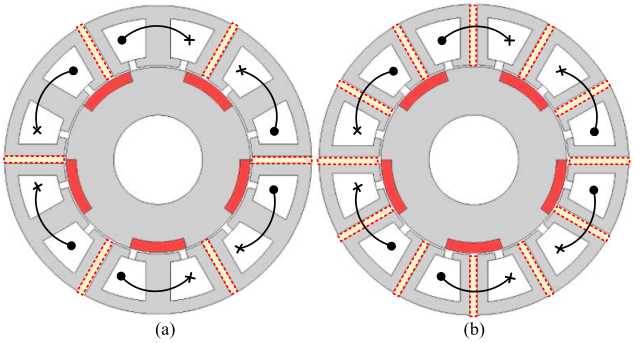

FIGURE 3. Cross sectional view of conventional CP (a) E-Core (b) C-Core.

TABLE 1. Depicted design specification for proposed IPMCPSM with modular H-type stator and rotor-CP.

Symbol	Value	Unit
R_s	13	mm
R_{bi}	11	mm
W_{PM}	3	mm
g	0.5	mm
S_{h1}	8.5	mm
S_{h2}	5.1	mm
FG	0-4	mm
W_{tb}	3.6	mm
W_{hb}	3.9	mm
H_s	17.5	mm
J_s	15	A/mm^2
N	180	-
PMs Remanence (B_r)	1.2	T
Stator outer diameter	90	mm
L_s	25	mm

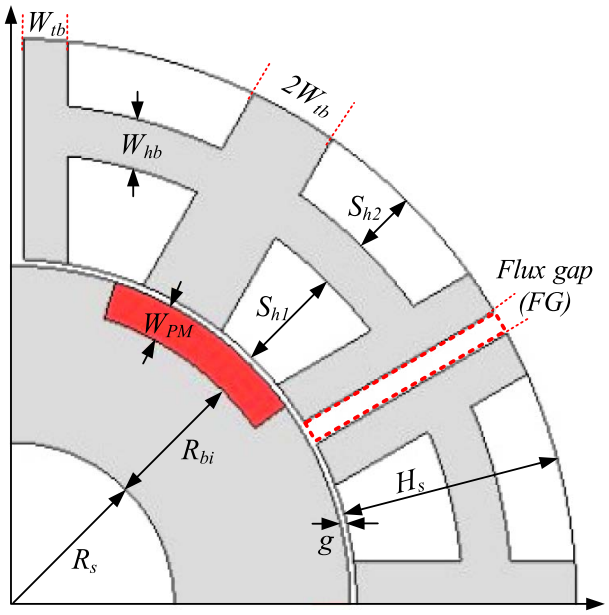

FIGURE 4. Design specification of proposed modular IPMCPSM.

tooth body, stack length, winding turns per phase, PM volume and height of the stator for both modular and non-modular are kept same for fair comparison. Thus, it is made sure that for fair comparison purpose, not only conventional but

also proposed modular/non-modular electric and magnetic loading remain same, whereas the possible stator slot (N_s) and rotor pole number (N_r) are computed as [25]

$$N_s = 2N_r + 2d \tag{1}$$

A simplified mathematical formulation explains working principle of the proposed IPMCPSM in both modular and non-modular form illustrates that considering rotor saliency with PM position and excitation, generated MMF is expressed as [33]

$$f_{pm}(\theta, t) = \sum_{i=1,2...}^{\infty} F_{pm_i} \cos\left[iN_r(\theta - \Omega_r t)\right] \tag{2}$$

where Ω_r, t and θ are rotational speed of rotor, time and mechanical position at stationary coordinate respectively whereas F_{pm_i} is i^{th}-order Fourier coefficients of generated MMF.

Air-gap permeance model considering effects of stator slot (N_{sr}) and rotor poles number in the form of Fourier series is expressed as

$$\Lambda_r(\theta, t) = \sum_{i=0,1...}^{\infty} \Lambda_{ri} \cos\left[iN_r(\theta - \Omega_r t)\right] \tag{3}$$

$$\Lambda_s(\theta, t) = \sum_{j=0,1...}^{\infty} \Lambda_{sj} \cos\left[jN_{sr}\theta\right] \tag{4}$$

whereas Λ_{ri} and Λ_{sj} are i^{th} and j^{th} order air-gap permeance Fourier coefficients respectively. It is noteworthy that air-gap permeance periodicity changes with the variation of N_{sr}, therefore, substitute with actual number of stator slot.

Utilizing MMF generated due to PM excitation and permeance of the air-gap, flux density in the air-gap is expressed as

$$B_{g-pm}(\theta, t) = f_{pm}(\theta, t)\,\Lambda_s(\theta, t) \tag{5}$$

$$= \sum_{i=1,2...}^{\infty} \sum_{j=0,1...}^{\infty} B_{pm_{(i,j)}} \times \cos\left[(iN_r \pm jN_{sr})\theta - iN_r\Omega_r t\right] \tag{6}$$

whereas the phase back-EMF as per flux density of the air-gap and phase winding function becomes

$$E_p(t) = -\frac{d}{dt}\left[R_g L_s \int_0^{2\pi} B_{g-pm}(\theta, t) N_{pwf}(\theta)\, d\theta\right] \tag{7}$$

whereas $R_g = R_s + R_{bi} + W_{pm}$, and $N_{pwf}(\theta)$ is phase winding function for single layer winding. For all and alternate pole winding function is expressed as

$$N_{pwf}(\theta) = \sum_{m=1,3,5...}^{\infty} N_{pwf_m} \cos(m\theta) \tag{8}$$

As per author in [16], higher order triplen harmonics of winding cancelled and the phase back-EMF with dominant

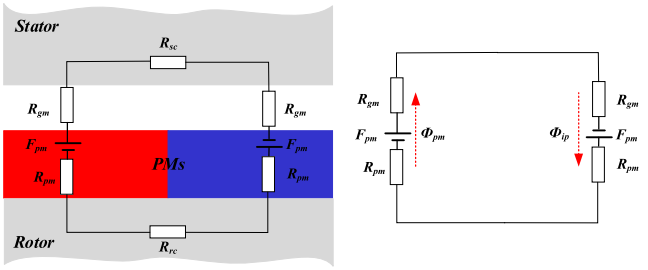

FIGURE 5. Simplified MEC model of conventional SMPM.

$|iN_r \pm jN_{sr}|$ order harmonics are

$$E_p(t) = R_g L_s \sum_{i=1,2...}^{\infty} \sum_{j=0,1,2...}^{\infty} \sum_{m=1,2,3...}^{m=|iN_r \pm jN_{sr}|} E_{p_{(i,j)}} \times \cos(iN_r\Omega_r t) \tag{9}$$

Analysis reveals that for IPMCPSM in C-core and H-core stator in non-modular and modular form, rotor pole pair i.e., ($N_r = 5$), and higher order harmonics contributing in back-EMF are analyzed in the proceeding sections.

III. ENHANCING CAPABILITY OF PROPOSED IPMCPSM

This section analyses enhancing capability of proposed IPMCPSMs in comparison with SMPMM machine utilizing magnetic equivalent circuit (MEC) model. In initial design phase both SMPMM and IPMCPSM utilizes same stator configuration, but different rotors as shown in Figure. 1(a) and Figure. 2(a) respectively. Enhancing capability is explained with analytical technique i.e., MEC with key assumptions as listed

1) Rotor and stator core permeance are infinite
2) End effect and leakage flux are neglected
3) Relative recoil permeability of PM is same as air-gap
4) PM is modeled as MMF source with series reluctance

In conventional SMPMM design, main magnetic flux paths are cumulative effect of North and South PM poles with opposite polarities forming MEC with two MMF source as shown in Figure. 5. In each magnetic pole, air-gap flux can be computed using MEC model as

$$\varphi_{g-SMPM} = \frac{2F_{pm}}{2R_{pm} + 2R_{gm} + R_{sc} + R_{rc}} \tag{10}$$

Utilizing the aforesaid assumption, air-gap flux for the MEC is modified as

$$\varphi_{g-SMPM} = \frac{2F_{pm}}{2R_{pm} + 2R_{gm}} \tag{11}$$

whereas F_{pm} is generated PM MMF, R_{pm} is PM magnetic reluctance, R_{sc} is stator core reluctance, R_{rc} is rotor core reluctance and R_{gm} is air-gap reluctance facing PM poles.

For proposed IPMCPSM, all North or south PMs Poles are replaced by salient iron pole which act as virtual PM poles and provide alternate magnetic flux path to the rest of PMs. It is notable that CP rotor configuration reduces half of the PM usage. From MEC model of IPMCPSM as shown in

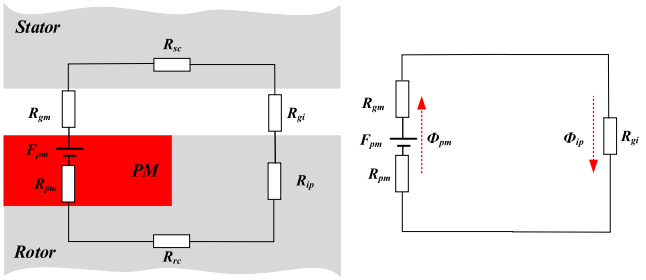

FIGURE 6. Simplified MEC model of proposed IPMCPSM.

Figure. 6, it can be clearly seen that PM MMF source is single and in each magnetic pole, air-gap flux can be computed as

$$\varphi_{g-IPMCPSM} = \frac{F_{pm}}{R_{pm} + R_{gm} + R_{gi} + R_{sc} + R_{rc}} \tag{12}$$

Based on above-mentioned assumption, air-gap flux for the MEC is modified as

$$\varphi_{g-IPMCPSM} = \frac{F_{pm}}{R_{pm} + R_{gm} + R_{gi}} \tag{13}$$

whereas R_{gi} is air-gap reluctance facing salient rotor iron pole.

Air-gap flux comparison of conventional SMPMM and proposed IPMCPSM shows that in IPMCPSMs, MMF source as well as reluctance of PM is reduced to half. This reduction is caused by saving PM consumption and doesn't lead in proportional reduction in air-gap flux. Thus, output electromagnetic performance is not significantly proportional. Therefore, CP rotor topologies increases PM utilization without proportional influence in electromagnetic performance. Moreover, due to salient iron rotor pole CP structure exploits reluctance torque and hence, improve torque density in IPMCPSMs. Detailed investigation of average torque and torque density is discussed in electromagnetic performance analysis with varying FGs and applied current angle.

IV. ELECTROMAGNETIC PERFORMANCE ANALYSIS

A. NO-LOAD ANALYSIS

Under no-load condition when no current is applied to armature winding, phase flux linkage, peak-to-peak-flux flux, back-EMF, cogging torque and harmonic spectra of flux linkage and back-EMF are thoroughly investigated under variable flux gaps to investigate the consequences of flux gap on key metric performance.

Phase flux linkage of IPMCPSM under varying FGs are as shown in Figure. 7 which reveals that with all pole flux gaps, it can be clearly seen that FGs have enhancing performance whereas for alternate pole flux gaps, there is negative impact on phase flux linkage and the peak values decreases. The increasing nature of phase flux linkage in case of all pole flux gap is visible in enlarge portion of Figure. 7(a) which is due to flux focusing effecting and enhancement of fundamental component of phase flux linkage as shown in Figure. 8. Despite of the increase in fundamental component of phase

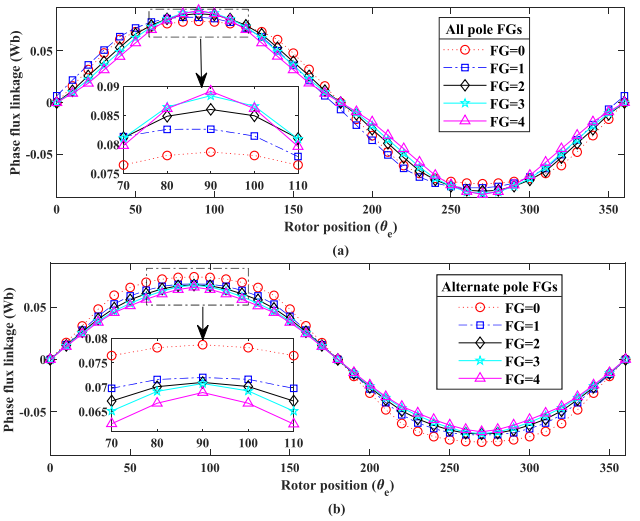

FIGURE 7. Phase flux linkage of proposed H-type stator core IPMCPSM with (a) All pole FGs and (b) Alternate pole FGs.

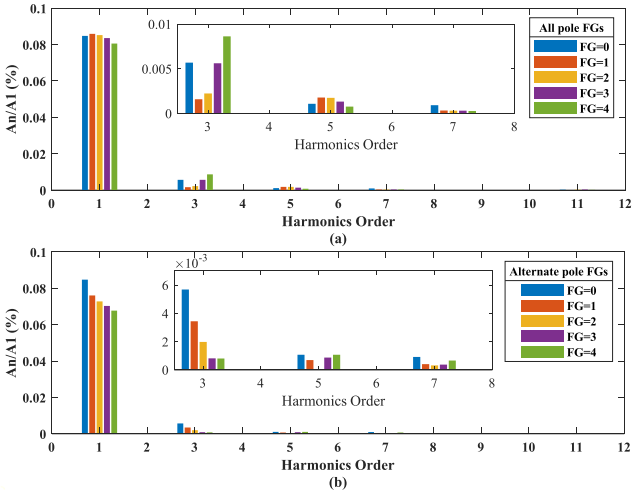

FIGURE 8. Harmonics spectra of phase flux linkage of proposed H-type stator core IPMCPSM with (a) All pole FGs and (b) Alternate pole FGs.

flux linkage, higher order harmonics continue to decrease with the increase in flux gaps resulting lower total harmonic distortion as shown in Figure. 9. It is noteworthy that in comparison of alternate pole FGs, THD of alternate pole FGs greatly increases with the increase in the FGs width which is contributing to working harmonics content that improve overall phase flux behaviour.

Furthermore, under no-load condition, consequence of varying flux gap on open-circuit induced back-EMF with harmonic spectra are shown in Figure. 10 and Figure. 11 respectively. It can be clearly seen that as soon as width of the flux gap continue to increase, the resultant induced back-EMF falls. In comparison with alternate pole flux gaps, all pole flux gap IPMCPSM with modular H-type stator core weaken effects of flux gap on phase back-EMF. Fundamental component of phase back-EMF as illustrated in Figure. 11 shows that for proposed IPMCPSM with all poles flux gaps,

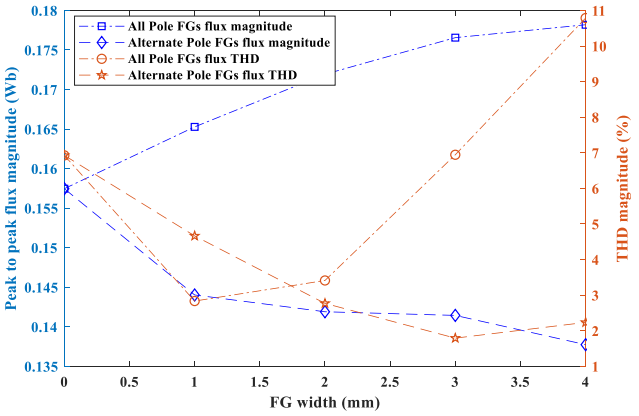

FIGURE 9. Variation of peak-to-peak magnitude of phase flux linkage and fundamental component of harmonics in proposed H-type stator core IPMCPSM with all pole and alternate pole FGs.

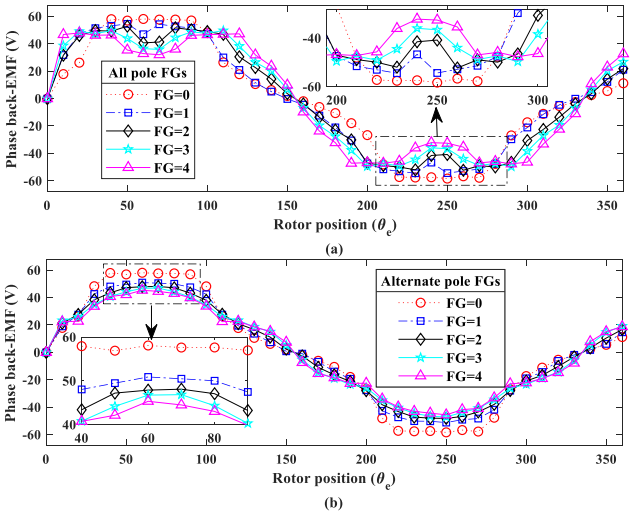

FIGURE 10. Back-EMF waveform for proposed H-type stator core IPMCPSM with (a) All pole FGs and (b) Alternate pole FGs.

back-EMF fundamental component increase in start and then decreases slightly whereas for alternate poles IPMCPSM, this fundamental component of phase back-EMF start to decrease with the increase in flux gap width. This analysis evident that flux gap has negative consequences in intriguing behaviours of modular IPMCPSM with alternate flux gaps.

It is worth mentioning that for phase back-EMF, amplitude of fundamental component increases with the increase in the flux gap that enhance flux focusing effects. This flux focusing effect can be achieved at feasible flux gap width. Based on the harmonic spectra of phase back-EMF as shown in Figure. 11, it can be clearly seen that for all pole flux gap, appropriate flux gap width of 0-2 mm results an improved flux focusing effects.

Despite of fundamental component, consequence of varying flux gap width contributing to back-EMF are $|iN_r \pm jN_{sr}|$ as illustrated in Table 2. This harmonics component varies with respect to rotor poles and stator slot combination. The

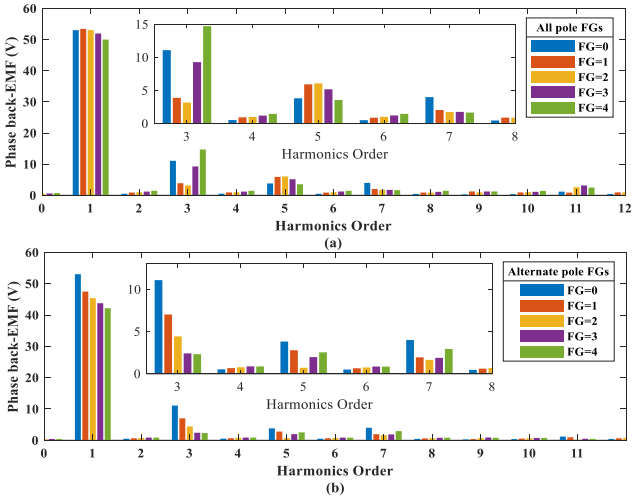

FIGURE 11. Harmonics spectra of back-EMF of proposed H-type stator core IPMCPSM with (a) All pole FGs and (b) Alternate pole FGs.

TABLE 2. harmonic order contributing in phase back-EMF.

Non-modular	Modular H-type stator core	
	Alternate pole FGs	All pole FGs
$\|5 \pm 12j\| =$ $5^{th}, 7^{th}, 19^{th}$ ...	$\|5 \pm 6j\| =$ $1^{th}, 5^{th}, 7^{th}$ ...	$\|5 \pm 12j\| =$ $5^{th}, 7^{th}, 19^{th}$ ...

higher order harmonics content such as 5^{th} and 7^{th} order is undesirable due to its contribution in torque ripples.

Comprehensive analysis of the harmonic spectra for all pole flux gaps reveals that dominant 5^{th} initially increase with flux gap of 1-2mm whereas it than decrease between 3-4 mm width whereas the 7^{th} order harmonic component continue to decrease. In case of alternate pole flux gap modular IPMCPSM, higher order harmonics (5^{th} and 7^{th}) first increases and then decreases. Not only torque ripple, but the aforesaid higher order harmonics have also influence on cogging torque which is shown in Figure. 12 and explained as per periodicity calculated as

$$LCM\left(k_p, N_s\right)/N_r \tag{14}$$

whereas $k_p = 1$, N_r and N_s are rotor pole number and stator slot.

This shows that torque periodicity of modular IPMCPSM with alternate pole flux gaps reduces to half in comparison with all pole flux gaps. Instantaneous cogging torque waveform for both all and alternate pole flux gaps IPMCPSM are shown in Figure. 12 whereas variation of the average torque and torque ripples are shown in Figure. 13.

B. ON-LOAD PERFORMANCE

Under loaded condition, proposed H-type modular IPMCPSM with varying flux gap width at all and alternate pole flux gap under rated current density of 15 A/mm^2 are investigated for average torque and torque ripple ratio as shown in Figure. 13. Analysis unveil that with the increase

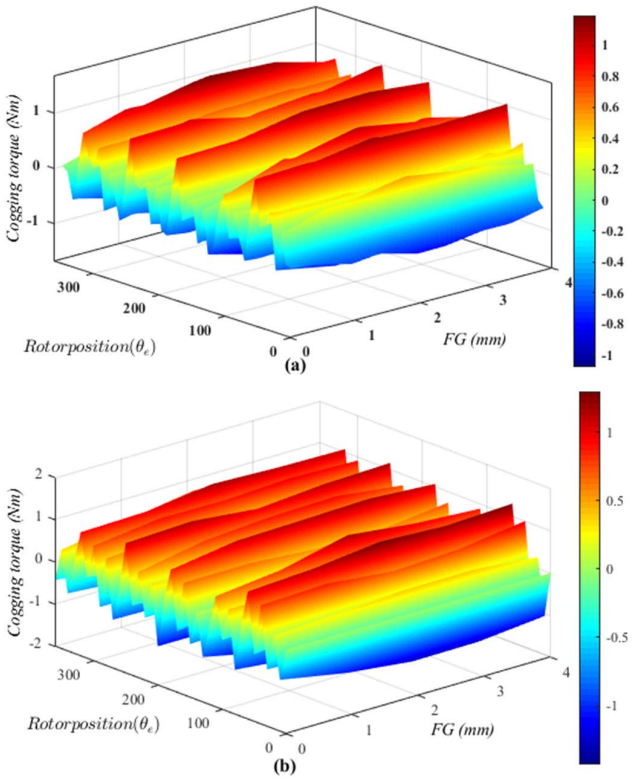

FIGURE 12. Influence of FGs on cogging torque in IPMCPSM with (a) All pole FGs and (b) Alternate pole FGs.

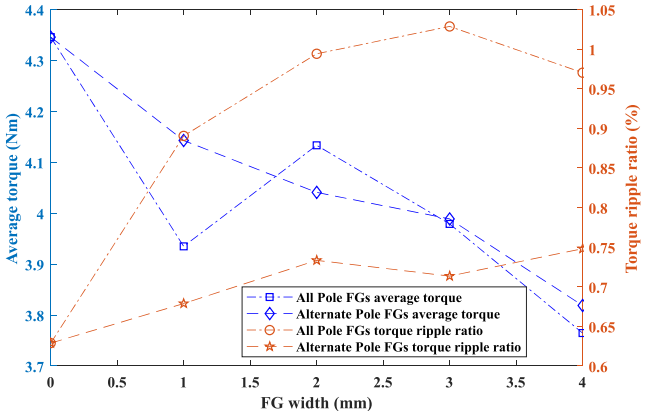

FIGURE 13. Torque characteristics of H-type modular IPMCPSM with varying FGs.

in the all-pole stator flux gap width not only average torque but also torque ripples decreases at first and then increases again. In case of alternate stator flux gap shows negative consequence on average torque and torque ripples in such a way that torque ripple ratio increases and average torque decreases. Again, this is due to dominancy of the higher order especially 5^{th} and 7^{th} harmonic in back-EMF.

It is noteworthy that in comparison with non-modular stator structure, the proposed modular stator with flux gaps varies air-gap permeance due to introduction of dummy slots through flux gaps that impact the core losses of machine as

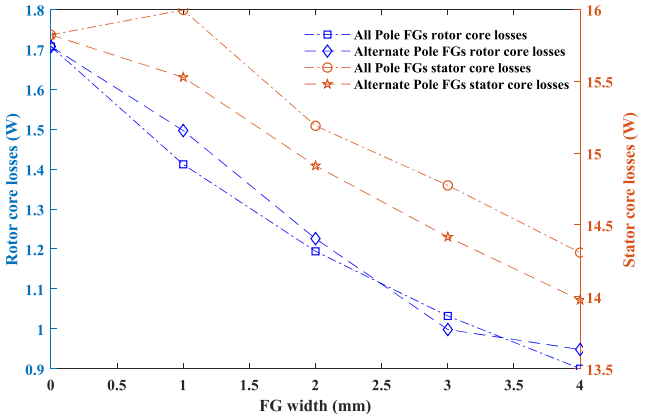

FIGURE 14. Influence of FGs on rotor and stator core losses.

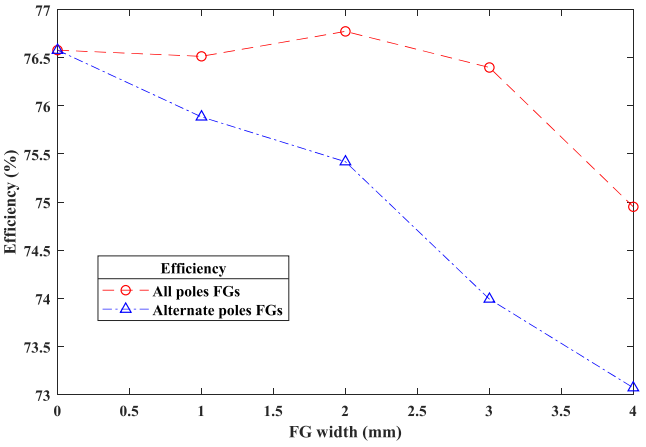

FIGURE 15. Effects of FGs width on efficiency @1200 rpm.

display in Figure. 14. In case of all pole flux gaps, the stator is formed of 12 modules whereas in case of alternate pole, it results 6 stator modules therefore, influence of the core losses in both cases significantly becomes dominant. Variation of the core losses under all pole and alternate pole stator flux gaps are shown in Figure. 14. It is evident that regardless of the rotor and stator pole combination, core losses continue to decrease in both types of the flux gaps. This reduction in core losses is due to suppression of higher order harmonics content and reduction of the mutual flux coupling at stator poles.

C. DYNAMIC PERFORMANCES ANALYSIS

Machine efficiency is key factor that play major role in dynamic analysis in design stage. Since modular structure are developed with variation of the stator flux gap at all and alternate stator pole that introduces dummy stator slots this results variation of the air-gap permeance that ultimately effect overall machine performance as well as efficiency therefore, detailed variation of the machine efficiency with variation of the flux gaps are computed as shown in Figure. 15. Analysis evident that in case of all pole stator flux gap, the proposed design show positive influence resulting

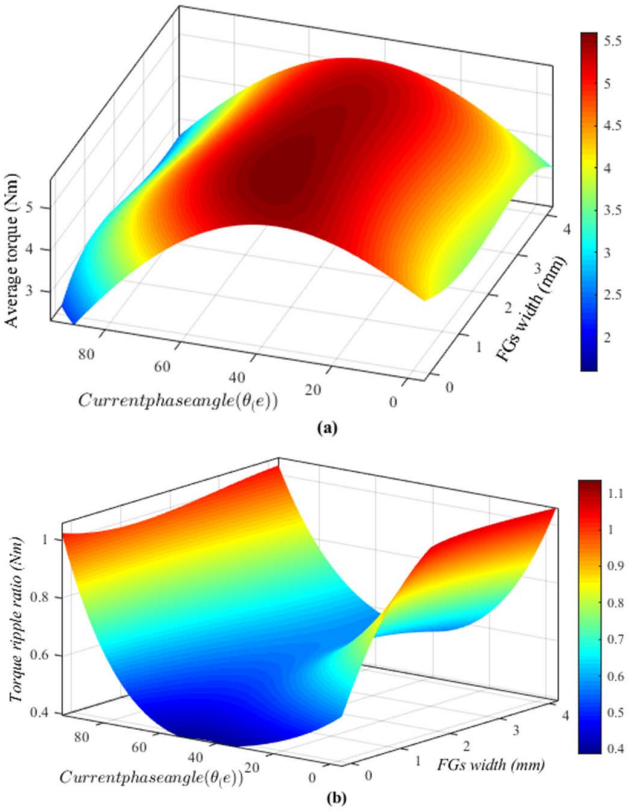

FIGURE 16. Torque characteristics of all pole FGs H-type stator IPMCPSM versus current phase angle of (a) Average torque and (b) torque ripple ratio.

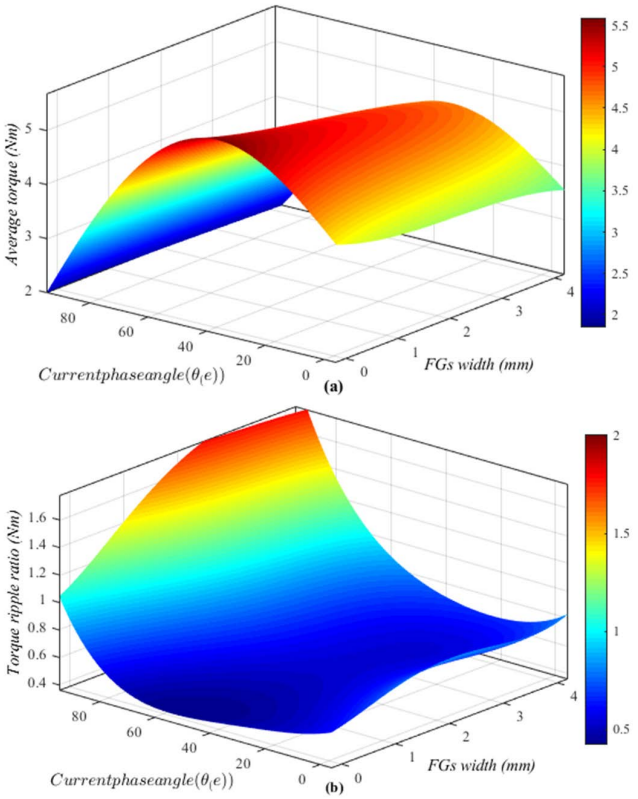

FIGURE 17. Torque characteristics of alternate pole FGs H-type stator IPMCPSM versus current phase angle of (a) Average torque and (b) torque ripple ratio.

slight increase in efficiency whereas for alternate stator pole flux gap, efficiency of machine decreases due to reduction of flux concentration of each phase.

In order to visualize the effect of advance current angle on output average torque, this part investigates influence of advance phase angle of applied current on average torque and torque ripples to sort out the optimum current angle that results maximum average torque and minimum torque ripples. This analysis is performed under various applied current with the advance phase shift at all and alternate stator flux gap as shown in Figure. 16 and Figure. 17, respectively.

From Figure. 16(a), analysis evident that for all pole stator flux gaps, with the increase in flux gaps width the resultant average torque response enhance. Moreover, this average torque profile improves with applied current phase angle. At the same time, from Figure. 16(b), it can be clearly seen that at this condition the torque ripples reach to minimum values. This analysis evident that maximum average torque and minimum torque ripple ratio for all pole flux gaps is achieved at 35-40 phase angle. Similarly, in case of alternate stator pole flux gaps, variation of the average torque and torque ripple ratio is shown in Figure. 17. Since, average torque improves with flux gaps, this results an improved torque density as well. Variation of the torque density profile for both all and alternate stator flux gaps are shown in

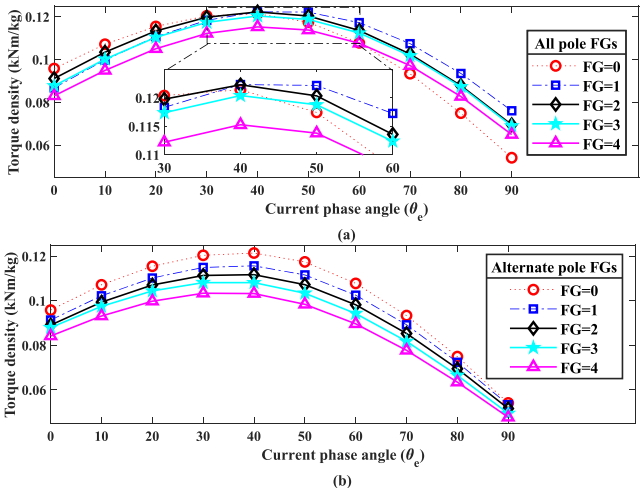

FIGURE 18. Torque density variation with current phase angle for (a) All pole FGs and (b) Alternate pole FGs.

Figure. 18. This analysis unveil that maximum torque density is achieved at the same advance phase angle (35-40 degree) where maximum average torque and minimum torque ripple is achieved.

Under dynamic performance analysis, variation of the flux gap on torque vs speed and power vs speed are investigated as illustrated in Figure. 19 and Figure. 20 respectively whereas efficiency map is illustrated in Figure 21 and Figure. 22.

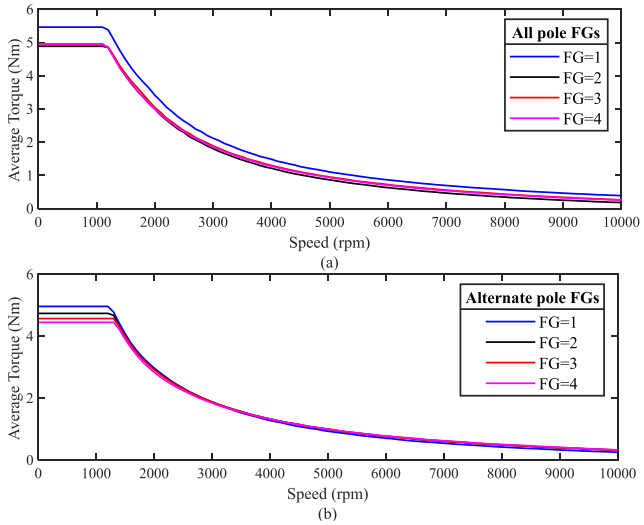

FIGURE 19. Torque versus speed curve for (a) All pole FGs and (b) Alternate pole FGs.

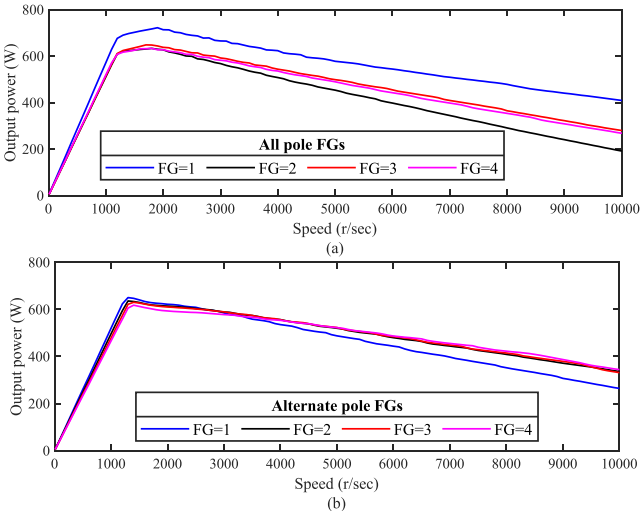

FIGURE 20. Power versus speed curve for (a) All pole FGs and (b) Alternate pole FGs.

Based on analysis, it is evident that due to higher phase flux linkage, flux gaps show slight influence on flux-weakening capability.

Furthermore, utilizing flux focusing merit of the proposed modular IPMCPSM with flux gaps, improved flux-weakening capability can be further achieved. It is noteworthy that in torque-speed and efficiency map, the average torque computed are slightly higher than the one reported in table 3 and table 4 due to consideration of the inverter setting and control technique.

D. FAULT-TOLERANT CAPABILITY

Magnetic flux density distribution in stator core varies with the introduction of the flux gaps that diverges magnetic flux

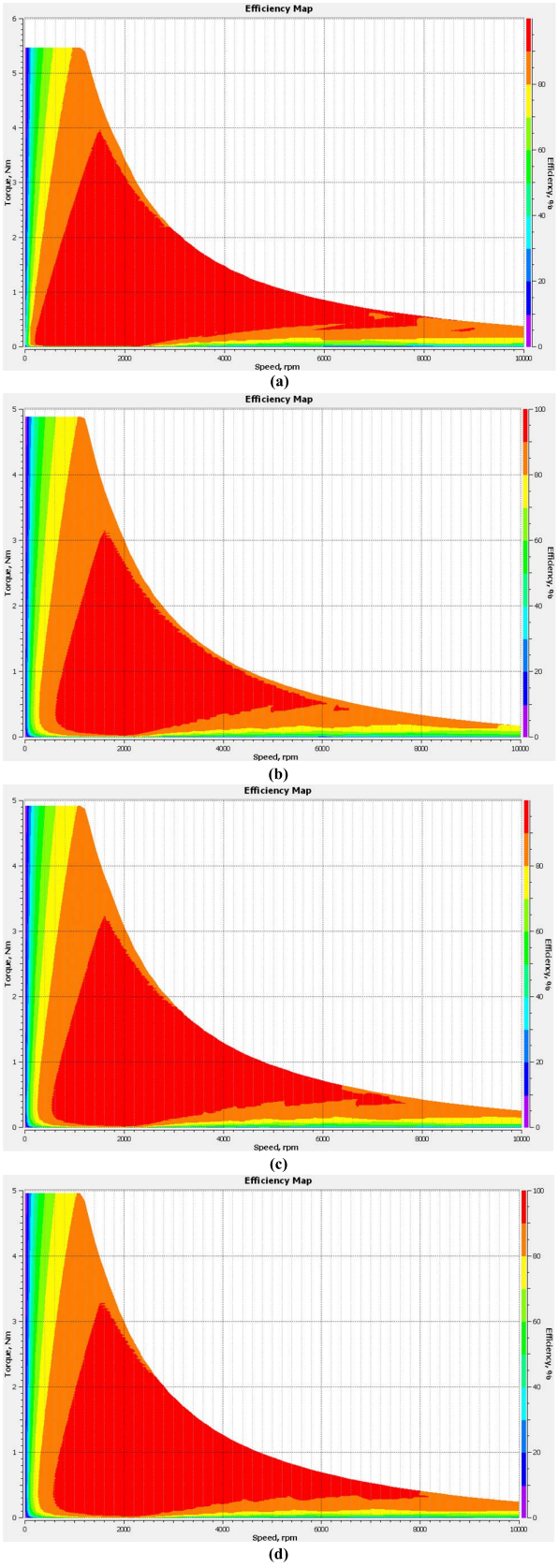

FIGURE 21. Efficiency map of proposed H-type IPMCPSM with all poles (a) FG=1 (b) FG=2 (c) FG=3 and (d) FG=4.

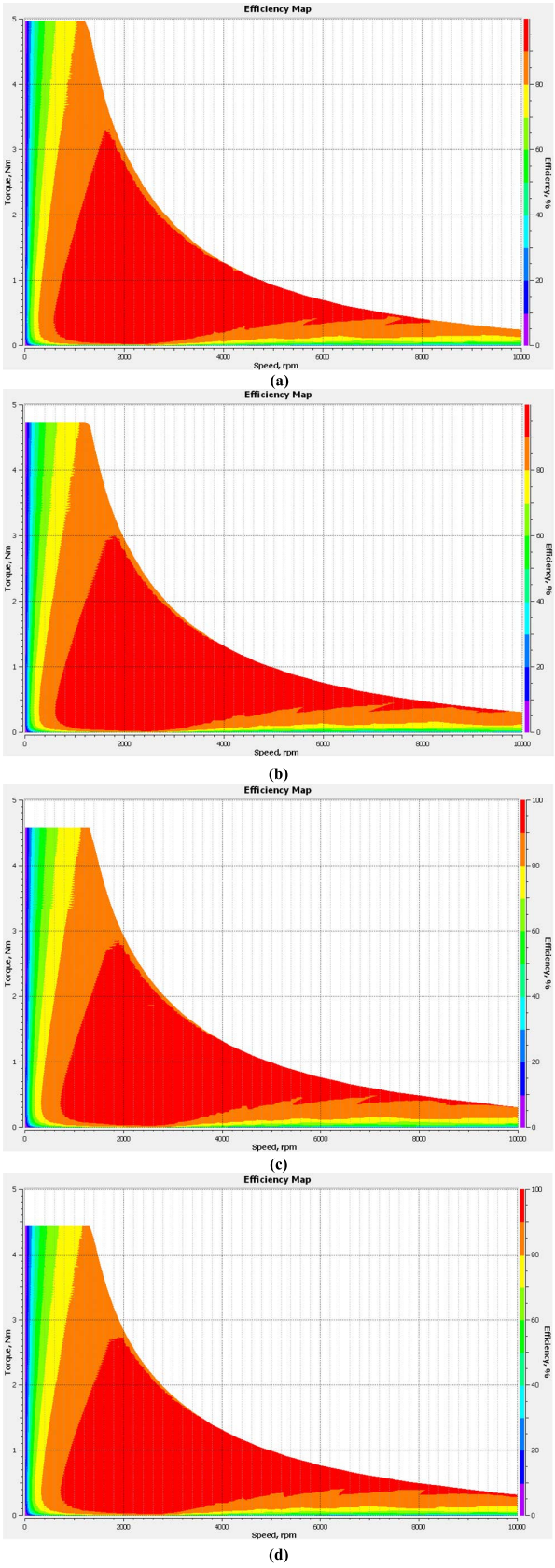

FIGURE 22. Efficiency map of proposed H-type IPMCPSM with alternate pole (a) FG=1 (b) FG=2 (c) FG=3 (d) FG=4.

TABLE 3. Quantitative electromagnetic performance of H-type stator with all teeth FGs @ speed=1200 rpm.

	Flux gap width					
Items	**0**	**1**	**2**	**3**	**4**	**Unit**
Φ	0.157	0.165	0.171	0.176	0.178	Wb
Φ_{THD}	6.92	2.83	3.41	6.94	10.78	%
EMF_{THD}	23.86	15.90	16.28	30.00	33.19	%
T_a	4.35	3.94	4.13	3.98	3.76	Nm
T_r	0.63	0.89	0.99	1.02	0.97	%
T_d	95.8	86.7	91.1	87.7	82.9	Nm/kg
P_d	16.81	15.92	16.42	16.07	15.53	kW/kg
R_{cl}	1.70	1.41	1.19	1.03	0.90	W
S_{cl}	15.82	15.99	15.19	14.77	14.30	W
η	76.57	76.51	76.77	76.39	74.95	%

TABLE 4. Quantitative electromagnetic performance of H-type stator with alternate teeth FGs @ speed=1200 rpm.

	Flux gap width					
Items	**0**	**1**	**2**	**3**	**4**	**Unit**
Φ	0.157	0.144	0.141	0.141	0.137	Wb
Φ_{THD}	6.92	4.66	2.76	1.79	2.23	%
EMF_{THD}	23.86	17.25	12.19	11.36	13.71	%
T_a	4.35	4.14	4.04	3.99	3.82	Nm
T_r	0.63	0.68	0.73	0.71	0.74	%
T_d	95.79	91.32	89.07	87.92	84.17	Nm/kg
P_d	16.84	16.31	16.01	15.85	15.40	kW/kg
R_{cl}	1.70	1.49	1.22	0.99	0.94	W
S_{cl}	15.82	15.52	14.91	14.41	13.97	W
η	76.57	75.88	75.41	73.99	73.07	%

path. This variation of magnetic flux paths decouples mutual flux that as a result both self and mutual inductance greatly varies. Therefore, self and mutual inductance are computed follow

$$L_i = \frac{\Phi_i - \Phi_o}{I_i} \tag{15}$$

$$M_{ij} = \frac{\Phi_j - \Phi_o}{I_i} \tag{16}$$

whereas L_i and M_{ij} are self and mutual inductance respectively, Φ_i, Φ_j, and Φ_o is self-phase flux linkage of phase i, and mutual-phase flux linkage of phase j, is phase flux linkage due to PMs, respectively whereas I_i is DC injected current in phase i.

For simplicity purpose, here only phase A is discussed whereas the rest of two phases will resemble phase A. Self and mutual inductance of phase A is computed at varying flux gap of stator by injecting a constant DC current to armature winding. The calculated self and mutual inductance at varying stator flux gap is display in Figure. 23 and Figure 24 respectively.

Analysis evident that with the change in rotor position and stator flux gap width, both self and mutual inductance varies. In case of all teeth stator flux gap, there is drastic variation in self-inductance whereas this variation in case of alternate teeth flux gaps is very slow due to dominancy of the mutual flux coupling. In the same way, with the variation of the flux gap in all teeth and alternate stator teeth, mutual inductance continues to decrease and approaches to zero due

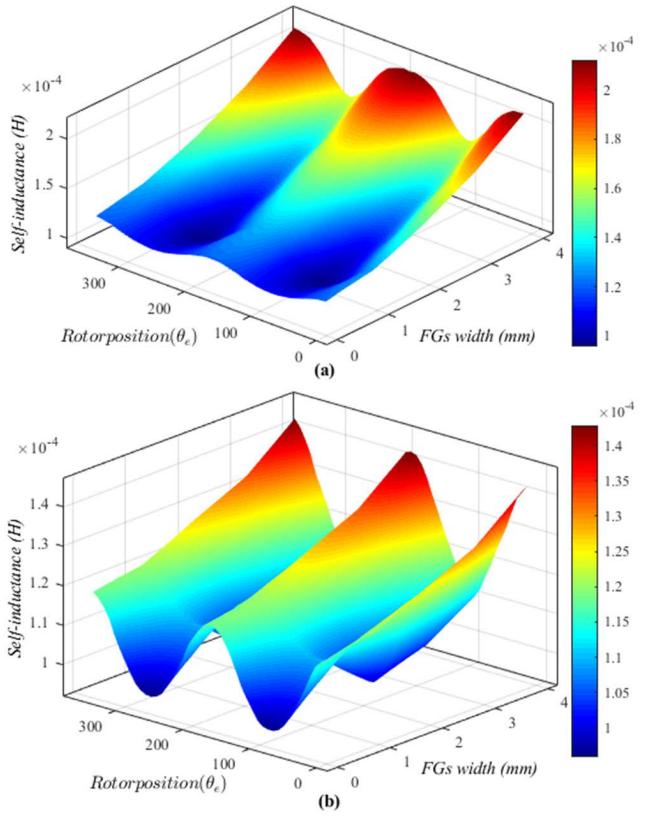

FIGURE 23. Influence of FGs on phase self-inductance for (a) All pole FGs and (b) Alternate pole FGs.

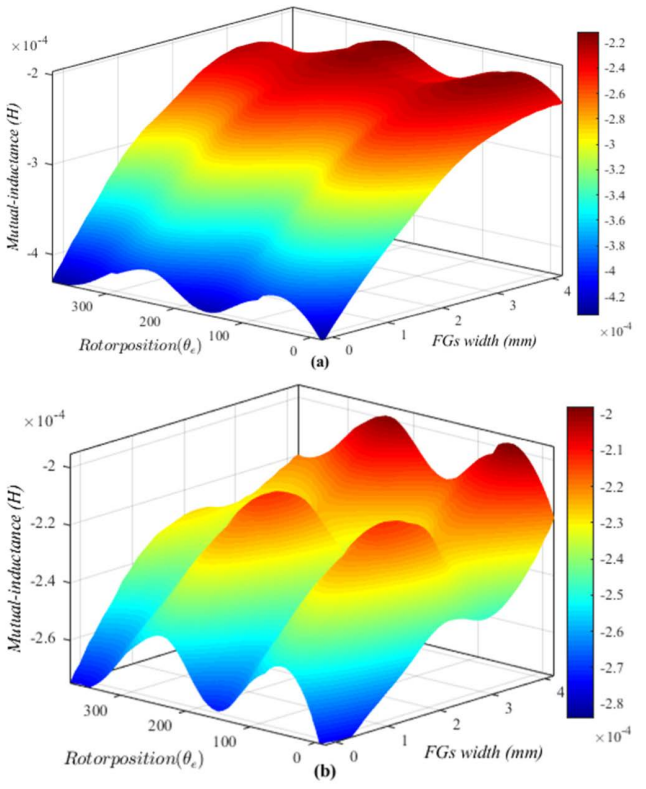

FIGURE 24. Influence of FGs on mutual inductance for (a) All pole FGs and (b) Alternate pole FGs.

to suppression and decoupling of mutual flux as shown in Figure. 25.

Thus, it is evident that introduction of flux gap in stator teeth results an increase in self-inductance and decrease in mutual inductance which greatly reduces the ratio of mutual to self-inductance resulting an improved fault tolerant capability because flux gaps physically isolate two adjacent phases thus, under fault condition, due to higher phase self-inductance, short circuit current is mitigated whereas due to low mutual-inductance, mutual effects of the faulty phase over healthy phase are truncated thus, offer improve fault tolerant capability. Furthermore, modular structure with stator flux gaps offers excellent stator colling in comparison with the conventional non-modular structure.

In addition, from Figure. 25 it is clear that due to partition of armature winding between the upper and lower stator slot, both winding contributes to the main flux i.e., inner armature fully incorporate however, outer stator slot winding contributes partially that results an improve performance in average torque. Furthermore, to achieve the target of higher average torque since the stator yoke is shortened in comparison with the conventional design (as shown in Fig. 25(a)), the flux path is shortened, due to which the reluctance is greatly reduced and contributes to achieve higher average torque.

V. CONVENTIONAL AND PROPOSED DESIGN

To justify usefulness of the proposed IPMCPSM with module stator with flux gap, performance analysis of conventional (E-core and C-core CP as shown in Figure. 3) and proposed design with key metric functions i.e., phase flux linkage (Φ), phase flux linkage THD (Φ_{THD}), back-EMF, back-EMF THD (EMF_{THD}), average torque (T_a), torque ripple ratio (T_r), torque density (T_d), power density (P_d), rotor core losses (R_{cl}), stator core losses (S_{cl}) and efficiency (η) is systematically compared. It is worth noting that modular H-type stator core and conventional C/E-core topology share same rotor-CP and stator dimension whereas different stator structure. The above-mentioned topologies of H-core, E-core and C-core are compared for varying FGs width as listed in table 3 to table 6 whereas waveform and harmonic spectra are shown in Figure. 26 to Figure. 30. Note that in this computation, influence of inverting rating and control technique is not taken into account due to which the average torque obtained is slightly lower than the one obtained in torque-speed curve and efficiency map.

From Figure. 26 and Figure. 27 it can be seen that flux gaps show positive impact on phase flux linkage of C-core structure which is mainly due to flux focusing effects on C-core which helps in improving flux weakening capability. Moreover, this increase in the phase flux linkage is due to reduction in the magnitude of 3rd order harmonics. Whereas FGs shows negative impact of E-core structure and magnitude of phase flux linkage decreases. In additional, comparing Φ_{THD}

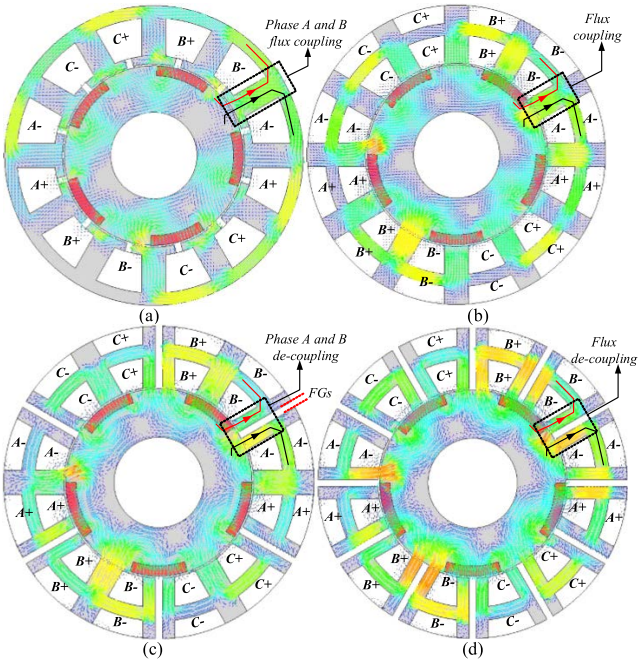

FIGURE 25. Magnetic flux lines distribution in novel H-type stator core (a) Non-modular conventional CP (C) Non-modular proposed H-type stator core (c) Modular H-type stator with alternate pole FGs and (d) Modular H-type stator with all pole FGs.

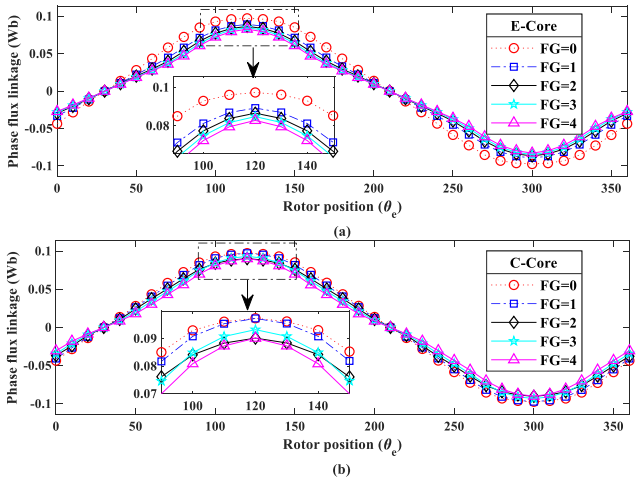

FIGURE 26. Phase flux linkage of conventional IPMCPSM with (a) E-core and (b) C-core.

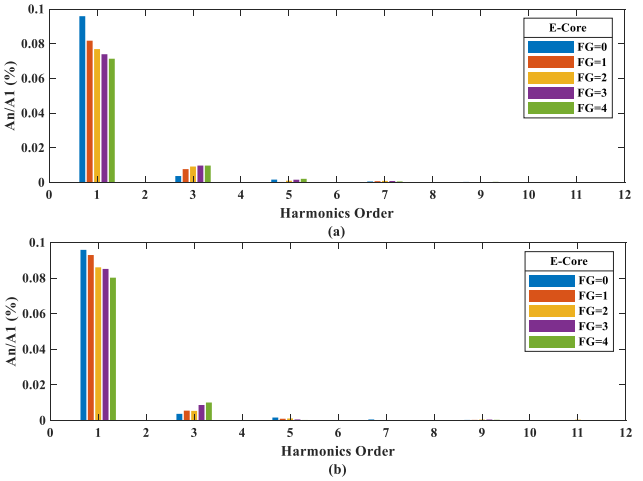

FIGURE 27. Harmonics spectra of phase flux linkage of conventional IPMCPSM with (a) E-core and (b) C-core.

TABLE 5. Quantitative electromagnetic performance of C-type stator core @ speed=1200 rpm.

Items	Flux gap width					Unit
	0	1	2	3	4	
Φ	0.194	0.194	0.180	0.186	0.180	Wb
Φ_{THD}	4.32	6.07	6.47	10.27	12.61	%
EMF_{THD}	15.47	19.05	21.08	31.30	37.90	%
T_a	1.63	2.12	2.14	2.22	2.10	Nm
T_r	1.40	1.20	1.15	1.18	1.29	%
T_d	35.93	46.78	47.17	49.00	46.50	Nm/kg
P_d	6.47	8.05	7.88	8.35	8.11	kW/kg
R_{cl}	1.95	0.601	0.444	0.415	0.372	W
S_{cl}	13.20	2.07	2.33	2.41	2.31	W
η	64.53	72.28	74.45	72.99	71.26	%

TABLE 6. Quantitative electromagnetic performance of E-type stator core @ speed=1200 rpm.

Items	Flux gap width					Unit
	0	1	2	3	4	
Φ	0.194	0.178	0.173	0.169	0.165	Wb
Φ_{THD}	4.32	9.49	12.11	13.44	14.03	%
EMF_{THD}	15.47	28.94	37.34	41.73	43.68	%
T_a	1.63	1.46	1.39	1.36	1.33	Nm
T_r	1.40	1.72	1.95	1.94	1.92	%
T_d	35.93	32.26	30.82	30.07	29.45	Nm/kg
P_d	6.47	6.05	5.89	5.83	5.77	kW/kg
R_{cl}	1.95	1.78	1.70	1.66	1.61	W
S_{cl}	13.20	14.69	14.19	13.76	13.42	W
η	64.53	60.94	59.72	58.98	58.35	%

from table 5 and table 6 for C-core and E-core, it can be seen that with the introduction in the FGs overall harmonics increases whereas for H-core stator structure as listed in table 3 and table 4 with the introduction of the FGs, the overall harmonics in phase flux linkage is effectively suppressed which is mainly due to structure variation of stator.

Quantitative performance analysis results that minimum Φ_{THD} for all pole FGs of H-core stator is 2.83% with $FG = 1$, whereas for alternate pole FGs minimum Φ_{THD} obtained is 1.79% with $FG = 3$. Comparing minimum Φ_{THD} of C-core and E-core which is 4.32%, it is concluded that all pole FGs H-core suppressed 52.6% and alternate pole FGs truncate up to 2.41 times.

Back-EMF and harmonic spectra for E-core and C-core CP is shown in Figure. 28 and Figure. 29 respectively. Analysis evident that with the placement of stator flux gap, amplitude of fundamental harmonic component declines that reduces peak to peak magnitude of back-EMF whereas and higher order harmonics increases which introduces harmonics. Comparing with back-EMF and harmonic spectra of H-core as shown in Figure. 10 and Figure. 11, it can be

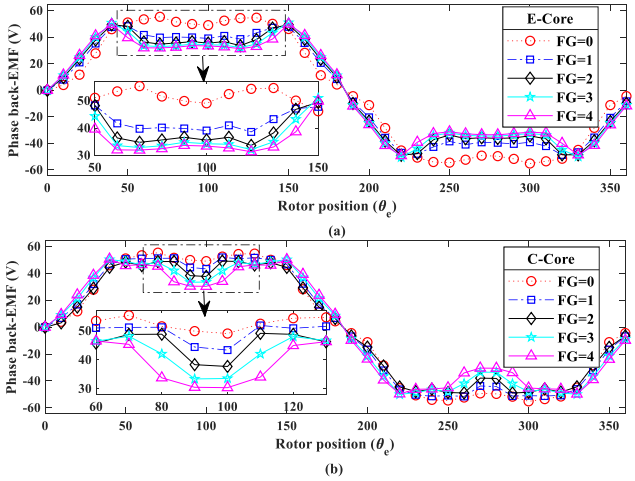

FIGURE 28. Back-EMF waveform of conventional IPMCPSM with (a) E-core and (b) C-core.

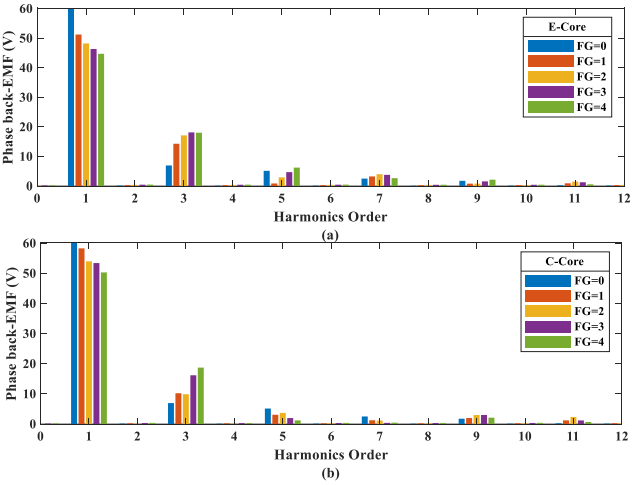

FIGURE 29. Harmonics spectra of back-EMF of conventional IPMCPSM with (a) E-core and (b) C-core.

seen that H-type IPMCPSM suppress higher order harmonic component reduces which suppress EMF_{THD}.

Performance analysis unveil that minimum EMF_{THD} for all teeth FGs of H-type modular stator core is 15.90% with $FG = 2$, whereas for alternate teeth FGs minimum EMF_{THD} obtained is 11.36% with $FG = 3$. Comparing with minimum EMF_{THD} of C-core and E-core which is 15.47%, analysis concluded that alternate teeth FGs H-core truncate 36.17% whereas in all teeth FGs it is increased by 2.7%.

In dynamic performance, efficiency (η) play major therefore compared for H-type, E-core and C-core as shown in Figure. 30 and listed in table 3 to table 6 for proposed and conventional design. From the analysis, it is concluded that FGs have positive impact on η with C-core whereas negative impact on E-core. With the introduction of FGs, η tend to reduce in E-core whereas for C-core, first it increases and then decreases. Quantitative performance analysis results that maximum η for all teeth FGs of H-core stator is 76.77% with $FG = 2$, whereas for alternate teeth FGs maximum η

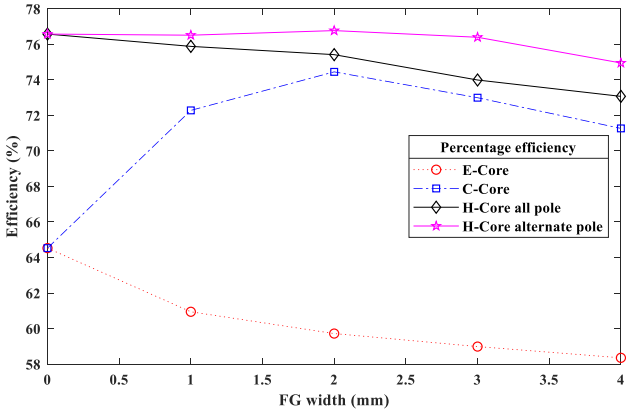

FIGURE 30. Comparison of efficiency for conventional E/C core and proposed H-type IPMCPSM with all teeth and alternate teeth FGs @ speed=1200 rpm.

obtained is 76.57% with $FG = 0$. Comparison with maximum C-core and E-core η of 74.45% and 64.53% respectively reveals that all teeth FGs H- core improve η by 3.1% and 18.96% whereas alternate teeth FGs increases η by 2.8% and 18.65% when compared with conventional C-core and E-core CP topologies.

Performance analysis reveals that highest T_a of H-type modular stator core is 4.35 Nm with $FG = 0$. Comparing with maximum T_a of C-core and E-core *i.e.* 2.2 Nm and 1.63 respectively, analysis concluded that H-core IPMCPSMs results T_a higher by 97.7% when compared with C-core and 2.66 times higher T_a when compared with E-core.

Quantitative analysis exposes that least T_r of H-type modular stator is 0.63% Nm. Comparing with lowest C-core and E-core T_r of 1.15% and 1.4% respectively, study expose that H-core diminish T_r by 45.21% and 55% when examined with C-core and E-core respectively. Similarly, comparing T_d and P_d of proposed H-type stator core with C-core and E-core CP topologies, analysis reveals that reveals that T_d and P_d to 2.66 and 2.59 times respectively.

To sum up, proposed H-type stator topologies of IPMCPSM results up to 2.45 times lower Φ_{THD}, 36.17% suppresses EMF_{THD}, improve η by 18.9%, diminish T_r up to 55% and boost T_a and P_d maximum up to 2.66, 2.59 times respectively with better flux focusing effects that improve flux weakening capability.

VI. CONCLUSION

In this paper novel H-type modular stator core IPMCPSM is investigated for static and dynamic performance with various stator flux gap width and compared with existing state of the art including E-core and C-core. Electromagnetic performance comparison of conventional and proposed design reveals that proposed IPMCPSM diminish EMF_{THD}, improve η by 18.9%, diminish T_r up to 55% and boost T_a and P_d maximum up to 2.66, 2.59 times respectively. Moreover, modular stator with flux gaps offers physical isolation of adjacent phases which results improved flux focusing effects to improve flux weakening capability and enhanced fault tolerant capability.

REFERENCES

[1] W. Ullah, F. Khan, and E. Sulaiman, "Sub-domain modelling and multi-variable optimisation of partitioned PM consequent pole flux switching machines," *IET Electr. Power Appl.*, vol. 14, no. 8, pp. 1360–1369, Aug. 2020.
[2] W. K. Ullah, S. Faisal, U. Erwan, U. Muhammad, and K. Noman, "Analytical validation of novel consequent pole E-core stator permanent magnet flux switching machine," *IET Electr. Power Appl.*, vol. 14, no. 5, pp. 789–796, May 2020.
[3] N. Ullah, F. Khan, W. Ullah, A. Basit, M. Umair, and Z. Khattak, "Analytical modelling of open-circuit flux linkage, cogging torque and electromagnetic torque for design of switched flux permanent magnet machine," *J. Magn.*, vol. 23, no. 2, pp. 253–266, Jun. 2018.
[4] J. Qi, Z. Q. Zhu, L. Yan, G. W. Jewell, C. W. Gan, Y. Ren, S. Brockway, and C. Hilton, "Suppression of torque ripple for consequent pole PM machine by asymmetric pole shaping method," in *Proc. IEEE Int. Electric Mach. Drives Conf. (IEMDC)*, Mar. 2021, pp. 1–7.
[5] J. Li, K. Wang, F. Li, S. S. Zhu, and C. Liu, "Elimination of even-order harmonics and unipolar leakage flux in consequent-pole PM machines by employing N-S-iron–S-N-iron rotor," *IEEE Trans. Ind. Electron.*, vol. 66, no. 3, pp. 1736–1747, Mar. 2019.
[6] J. Li, K. Wang, and C. Liu, "Comparative study of consequent-pole and hybrid-pole permanent magnet machines," *IEEE Trans. Energy Convers.*, vol. 34, no. 2, pp. 701–711, Jun. 2019.
[7] R. Zhou, G. J. Li, K. Zhang, Z. Q. Zhu, M. P. Foster, and D. A Stone, "Performance investigation of consequent-pole PM machines with E-core and C-core modular stators," *IEEE Trans. Energy Convers.*, vol. 36, no. 6, pp. 1169–1179, Sep. 2020, doi: 10.1109/TEC.2020.3027366.
[8] J. Li, K. Wang, and C. Liu, "Torque improvement and cost reduction of permanent magnet machines with a dovetailed consequent-pole rotor," *IEEE Trans. Energy Convers.*, vol. 33, no. 4, pp. 1628–1640, Dec. 2018.
[9] B. Ren, G. Li, Z. Q. Zhu, M. Foster, and D. Stone, "Performance comparison between consequent-pole and inset modular permanent magnet machines," *J. Eng.*, vol. 2019, no. 17, pp. 3951–3955, Jun. 2019.
[10] Y. Wang, Z.-Q. Zhu, J. Feng, S. Guo, Y. Li, and Y. Wang, "Investigation of unbalanced magnetic force in fractional-slot permanent magnet machines having an odd number of stator slots," *IEEE Trans. Energy Convers.*, vol. 35, no. 4, pp. 1954–1963, May 2020.
[11] Z. Liang, Y. Gao, D. Li, and R. Qu, "Design of a novel dual flux modulation machine with consequent-pole spoke-array permanent magnets in both stator and rotor," *CES Trans. Elect. Mach. Syst.*, vol. 2, no. 1, pp. 73–81, Mar. 2018.
[12] H. Hua, Z. Q. Zhu, and H. Zhan, "Novel consequent-pole hybrid excited machine with separated excitation stator," *IEEE Trans. Ind. Electron.*, vol. 63, no. 8, pp. 4718–4728, Apr. 2016.
[13] S. U. Chung, J. W. Kim, B. C. Woo, D. K. Hong, J. Y. Lee, and D. H. Koo, "A novel design of modular three-phase permanent magnet Vernier machine with consequent pole rotor," *IEEE Trans. Magn.*, vol. 47, no. 10, pp. 4215–4218, Sep. 2011.
[14] Z. Z. Wu and Z. Q. Zhu, "Partitioned stator flux reversal machine with consequent-pole PM stator," *IEEE Trans. Energy Convers.*, vol. 30, no. 4, pp. 1472–1482, Dec. 2015.
[15] J. Asama, M. Amada, M. Takemoto, A. Chiba, T. Fukao, and A. Rahman, "Voltage characteristics of a consequent-pole bearingless PM motor with concentrated windings," *IEEE Trans. Magn.*, vol. 45, no. 6, pp. 2823–2826, Jun. 2009.
[16] J. Amemiya, A. Chiba, D. G. Dorrell, and T. Fukao, "Basic characteristics of a consequent-pole-type bearingless motor," *IEEE Trans. Magn.*, vol. 41, no. 1, pp. 82–89, Jan. 2005.
[17] M. Nakagawa, Y. Asano, A. Mizuguchi, A. Chiba, C. X. Xuan, M. Ooshima, and D. G. Dorrell, "Optimization of stator design in a consequent-pole type bearingless motor considering magnetic suspension characteristics," *IEEE Trans. Magn.*, vol. 42, no. 10, pp. 3422–3424, Oct. 2006.
[18] Y. Gao, R. Qu, D. Li, J. Li, and G. Zhou, "Consequent-pole flux-reversal permanent-magnet machine for electric vehicle propulsion," *IEEE Trans. Appl. Supercond.*, vol. 26, no. 4, pp. 1–5, Jun. 2016.
[19] S.-U. Chung, J.-W. Kim, Y.-D. Chun, B.-C. Woo, and D.-K. Hong, "Fractional slot concentrated winding PMSM with consequent pole rotor for a low-speed direct drive: Reduction of rare Earth permanent magnet," *IEEE Trans. Energy Convers.*, vol. 30, no. 1, pp. 103–109, Mar. 2015.
[20] J. Li and K. Wang, "Analytical determination of optimal PM-arc ratio of consequent-pole permanent magnet machines," *IEEE Trans. Magn.*, vol. 23, no. 5, pp. 2168–2177, Oct. 2018.
[21] L. Zhang, K. Wang, J. Li, and F. Li, "Comparison study of interior permanent magnet synchronous machine with conventional and consequent pole rotor," in *Proc. 22nd Int. Conf. Electr. Mach. Syst. (ICEMS)*, Harbin, China, Aug. 2019, pp. 1–5.
[22] Q. Wang, S. Niu, and X. Luo, "A novel hybrid dual-PM machine excited by AC with DC bias for electric vehicle propulsion," *IEEE Trans. Ind. Electron.*, vol. 64, no. 9, pp. 6908–6919, Sep. 2017.
[23] F. Li, K. Wang, J. Li, and H. J. Zhang, "Suppression of even-order harmonics and torque ripple in outer rotor consequent-pole PM machine by multilayer winding," *IEEE Trans. Magn.*, vol. 54, no. 11, pp. 1–5, Jun. 2018.
[24] J. Li, K. Wang, and H. Zhang, "Flux-focusing permanent magnet machines with modular consequent-pole rotor," *IEEE Trans. Ind. Electron.*, vol. 67, no. 5, pp. 3374–3385, May 2020.
[25] G. J. Li, Z. Q. Zhu, W. Q. Chu, M. P. Foster, and D. A. Stone, "Influence of flux gaps on electromagnetic performance of novel modular PM machines," *IEEE Trans. Energy Convers.*, vol. 29, no. 3, pp. 716–726, Apr. 2014.
[26] W. Ullah, F. Khan, M. Umair, and B. Khan, "Analytical methodologies for design of segmented permanent magnet consequent pole flux switching machine: A comparative analysis," *COMPEL-Int. J. Comput. Math. Electr. Electron. Eng.*, vol. 40, no. 3, pp. 744–767, Aug. 2021.
[27] W. Ullah, F. Khan, E. Sulaiman, I. Sami, and J.-S. Ro, "Analytical subdomain model for magnetic field computation in segmented permanent magnet switched flux consequent pole machine," *IEEE Access*, vol. 9, pp. 3774–3783, 2021.
[28] C. Peng, D. Wang, Z. Feng, and B. Wang, "A new segmented rotor to mitigate torque ripple and electromagnetic vibration of interior permanent magnet machine," *IEEE Trans. Ind. Electron.*, vol. 69, no. 2, pp. 1367–1377, Feb. 2021.
[29] N. J. Baker, D. J. B. Smith, M. C. Kulan, and S. Turvey, "Design and performance of a segmented stator permanent magnet alternator for aerospace," *IEEE Trans. Energy Convers.*, vol. 33, no. 1, pp. 40–48, Mar. 2018.
[30] J. Zhao, W. Fu, Y. Zheng, Z. Chen, and Y. Wang, "Comparative study of modular-stator and conventional outer-rotor flux-switching permanent-magnet motors," *IEEE Access*, vol. 7, pp. 38297–38305, 2019.
[31] W. Ullah, F. Khan, N. Ullah, and A. Majid, "Investigation of third harmonic utilization for torque performance improvement in novel H-type modular stator consequent pole machine," *Electr. Eng.*, pp. 1–13, Feb. 2022.
[32] W. Ullah and F. Khan, "Design and performance analysis of a novel outer-rotor consequent pole permanent magnet machine with H-type modular stator," *IEEE Access*, vol. 9, pp. 125331–125341, 2021.
[33] S. Cai, Z.-Q. Zhu, C. Wang, J.-C. Mipo, and S. Personnaz, "A novel fractional slot non-overlapping winding hybrid excited machine with consequent-pole PM rotor," *IEEE Trans. Energy Convers.*, vol. 35, no. 3, pp. 1628–1637, Sep. 2020.

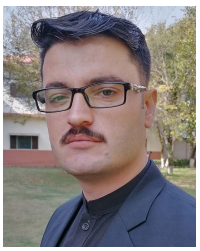

WASIQ ULLAH (Graduate Student Member, IEEE) was born in Peshawar, Khyber Pakhtunkhwa, Pakistan, in 1995. He received the B.S. and M.S. degrees in electrical (power) engineering from COMSATS University Islamabad (Abbottabad Campus), Abbottabad, Pakistan, in 2018 and 2020, respectively, where he is currently pursuing the Ph.D. degree in electrical (power) engineering.

Since 2018, he has been a Research Associate with the Electric Machine Design Research Laboratory. His research interests include analytical modeling, design analysis and optimization of permanent magnet flux switching machines, linear flux switching machines, hybrid excited flux switching machines, novel consequent pole flux switching machines for high-speed brushless AC applications, and flux switching generators for counter-rotating wind turbines applications.

Mr. Ullah is basically from Afghanistan and serve as a Reviewer for IEEE Access, *IET Electric Power Application, MDPI Journals*, and 2022 IEEE Energy Conversion Congress and Exposition (ECCE 2022). He is a member of IEEE-IES Electrical Machines Technical Committee Members and a member of Pakistan Engineering Council.

FAISAL KHAN (Senior Member, IEEE) was born in Charsadda, Khyber Pakhtunkhwa, Pakistan, in 1986. He received the B.S. degree in electronics engineering and the M.S. degree in electrical engineering from COMSATS University Islamabad (Abbottabad Campus), Pakistan, in 2009 and 2012, respectively, and the Ph.D. degree in electrical engineering from Universiti Tun Hussein Onn Malaysia, Malaysia, in 2017.

From 2010 to 2012, he was a Lecturer with the University of Engineering & Technology, Abbottabad, Pakistan. Since 2017, he has been an Assistant Professor with the Electrical and Computer Engineering Department, COMSATS University Islamabad (Abbottabad Campus). He is currently the Head of the Electric Machine Design Research Laboratory, and the author of more than 100 publications, one patent, and received multiple research awards. His research interests include design and analysis of flux-switching machines, synchronous machines, and DC machines.

He is a member of IEEE-IES Electrical Machines Technical Committee.

SHAHID HUSSAIN (Graduate Student Member, IEEE) was born in Swabi, Khyber Pakhtunkhwa, Pakistan. He received the B.S. degree in electrical power engineering from COMSATS University Islamabad, Abbottabad Campus, Abbottabad, Pakistan, in 2019, where he is currently pursuing the M.S. degree in electrical power engineering. He has been a Research Assistant with the Electric Machine Design Research Laboratory, since 2020. His research interests include design analysis, optimization and experimental validation of modular, and complementary fault tolerant field excited linear flux switching machines for long stroke application. He is a member of Pakistan Engineering Council.

FAHAD ALTURISE received the Ph.D. degree in information technology from Flinders University. He is currently working as an Associate Professor with the Computer Department, College of Science and Arts in Ar Rass, Qassim University, Saudi Arabia. He has an experience of 12 years in the field of teaching and research. He has published 12 articles in international journals/conference proceedings. His primary research interest includes e-learning, e-services, e-government, the IoT, ICT adaption, IT security, and software engineering. He was a member of the Australian Computer Society (ACS) for four years.

MUHAMMAD YOUSUF (Graduate Student Member, IEEE) received the B.S. degree in electrical engineering (electronics) from the Federal Urdu University of Arts Science and Technology (FUUAST) Islamabad, Pakistan, in 2015, and the M.S. degree in electrical engineering from COMSATS University Islamabad, Islamabad, in 2019. He is currently pursuing the Ph.D. degree in electrical engineering with COMSATS University Islamabad, (Abbottabad Campus), Abbottabad, Pakistan. His research interests include design, analysis and optimization of permanent magnet flux switching machines, multi-phase machines, and axial flux permanent magnet machines.

SIDDIQUE AKBAR was born in Khyber Pakhtunkhwa, Pakistan, in 1997. He received the bachelor's degree in electrical (power) engineering from COMSATS University Islamabad, Abbottabad Campus, Pakistan, in 2020, where he is currently pursuing the M.S. degree in electrical engineering. He has been a Research Assistant with the Electric Machine Design Research Laboratory, since 2020. His research interests include analysis, optimization and experimental validation of actuator, and flux switching machines.